

# Global phase diagram and quantum spin liquids in spin-1/2 triangular antiferromagnet

Shou-Shu Gong<sup>1</sup>, W. Zhu<sup>2</sup>, J.-X. Zhu<sup>2,3</sup>, D. N. Sheng<sup>4</sup>, and Kun Yang<sup>5</sup>

<sup>1</sup>National High Magnetic Field Laboratory, Florida State University, Tallahassee, FL 32310

<sup>2</sup>Theoretical Division, T-4 and CNLS, Los Alamos National Laboratory, Los Alamos, NM 87545

<sup>3</sup>Center for Integrated Nanotechnologies, Los Alamos National Laboratory, Los Alamos, NM 87545

<sup>4</sup>Department of Physics and Astronomy, California State University, Northridge, CA 91330

<sup>5</sup>National High Magnetic Field Laboratory and Department of Physics, Florida State University, Tallahassee, FL 32306

We study the spin-1/2 Heisenberg model on the triangular lattice with the nearest-neighbor  $J_1 > 0$ , the next-nearest-neighbor  $J_2 > 0$  Heisenberg interactions, and the additional scalar chiral interaction  $J_\chi(\vec{S}_i \times \vec{S}_j) \cdot \vec{S}_k$  for the three spins in all the triangles using large-scale density matrix renormalization group calculation on cylinder geometry. With increasing  $J_2$  ( $J_2/J_1 \leq 0.3$ ) and  $J_\chi$  ( $J_\chi/J_1 \leq 1.0$ ) interactions, we establish a quantum phase diagram with the magnetically ordered  $120^\circ$  phase, stripe phase, and non-coplanar tetrahedral phase. In between these magnetic order phases, we find a chiral spin liquid (CSL) phase, which is identified as a  $\nu = 1/2$  bosonic fractional quantum Hall state with possible spontaneous rotational symmetry breaking. By switching on the chiral interaction, we find that the previously identified spin liquid in the  $J_1 - J_2$  triangular model ( $0.08 \lesssim J_2/J_1 \lesssim 0.15$ ) shows a phase transition to the CSL phase at very small  $J_\chi$ . We also compute spin triplet gap in both spin liquid phases, and our finite-size results suggest large gap in the odd topological sector but small or vanishing gap in the even sector. We discuss the implications of our results to the nature of the spin liquid phases.

PACS numbers: 73.43.Nq, 75.10.Jm, 75.10.Kt

## I. INTRODUCTION

Quantum spin liquid (QSL) is one kind of long-range entangled states with fractionalized quasiparticles<sup>1</sup>. Since the proposal by P. W. Anderson, the concept of QSL has been playing an important role for understanding strongly correlated materials and unconventional superconductors<sup>2</sup>. Although QSLs have been pursued for more than two decades<sup>3-9</sup>, only recently such novel states have been found in realistic spin models<sup>10-23</sup>, in which geometric frustration and competing interactions play important roles for developing spin liquid states.

One of the most promising spin liquid candidates is the antiferromagnet on the corner-sharing kagome lattice. Experimentally, spin liquid-like behaviors have been observed in several kagome materials such as herbertsmithite<sup>24-28</sup>. Theoretically, the most extensively studied kagome model is the spin-1/2 kagome Heisenberg model with the nearest-neighbor (NN) interaction. Thanks to the recent large-scale Density Matrix Renormalization Group (DMRG) simulations<sup>29,30</sup>, conventional orders have been excluded, leading to a QSL ground state. However, the nature of this spin liquid is still in debate. DMRG calculations suggest a gapped spin liquid<sup>29-31</sup>, seemingly consistent with a  $Z_2$  topological order<sup>30,31</sup>. Recent tensor network state simulations identify the  $Z_2$  topological order of the obtained variational wavefunction<sup>32</sup>, but so far the four degenerate ground states of the putative  $Z_2$  QSL have not been found in exact diagonalization (ED)<sup>33,34</sup> and DMRG calculations, leaving this problem open. On the other hand, variational studies based on the fermionic parton wavefunctions find the gapless U(1) Dirac spin liquid rather than the gapped  $Z_2$  spin liquid with the optimized variational energy<sup>35-37</sup>. Very recently, tensor renormalization group<sup>38,39</sup> and DMRG<sup>40</sup> calculations also suggest the gapless spin liquid as a strong candidate. Interestingly, studies on the modified kagome models<sup>14-16,41-43</sup> find that the kagome spin li-

quid emerges near the phase boundaries of several ordered phases, suggesting possible strong competitions of the different physics in the kagome spin liquid regime. In particular, a fully gapped chiral spin liquid (CSL)<sup>44,45</sup> is found by switching on small further-neighbor<sup>15,16</sup> or chiral interactions<sup>14</sup> on the NN kagome model.

Another promising spin liquid candidate is the antiferromagnet on the edge-sharing triangular lattice. Although frustration is present in the spin-1/2 NN triangular model, it turns out to still exhibit a  $120^\circ$  antiferromagnetic order<sup>46,47</sup>. In the recent experiments on the triangular organic Mott insulators such as  $\kappa$ -(ET)<sub>2</sub>Cu<sub>2</sub>(CN)<sub>3</sub> and EtMe<sub>3</sub>Sb[Pd(dmit)<sub>2</sub>]<sub>2</sub><sup>48-52</sup>, spin liquid-like behaviors have been found. Theoretically, multi-spin exchange interactions, which can lead to the gapless spin Bose metal with a large spinon Fermi surface<sup>53-55</sup> and the gapless spin liquid with a quadratic band touching<sup>56,57</sup> depending on the strength of interaction, and the space anisotropic interaction<sup>58-61</sup> have been suggested to understand the spin-liquid behaviors in triangular materials.

Recently, a new spin liquid phase is found in the spin-1/2 triangular Heisenberg model with the NN  $J_1$  and the next-nearest-neighbor (NNN)  $J_2$  interactions for  $0.08 \lesssim J_2/J_1 \lesssim 0.15$ , which is sandwiched by a  $120^\circ$  magnetic phase and a stripe magnetic order phase<sup>56,62-67</sup>. This frustrating  $J_2$  interaction is considered as a possible mechanism to understand the spin-liquid behaviors of the newly synthesized triangular materials YbMgGaO<sub>4</sub><sup>68</sup> and Ba<sub>3</sub>InIr<sub>2</sub>O<sub>9</sub><sup>69</sup>. For this  $J_1 - J_2$  model, DMRG calculations on cylinder system find the evidence of spin liquid including the two near-degenerate ground states in the even and odd topological sectors whose energy difference decays rapidly with growing cylinder width, and the fractionalized spin-1/2 quasiparticle revealed by inserting flux simulation and entanglement spectrum (ES)<sup>64-66</sup>. On the finite-size DMRG calculations, the spin triplet gap measured above the overall ground state (in the odd sector) is big

( $\Delta_T \sim 0.3J_1$ )<sup>64,65</sup>, seemingly consistent with a gapped spin liquid<sup>70,71</sup>. Nonetheless, the even and odd sectors show some distinct features in finite-size DMRG calculation. While the odd sector shows a short correlation length that could be consistent with the large gap, the even sector exhibits a much larger one<sup>65,66</sup>, which may suggest smaller gap in the even sector. The low-lying entanglement spectrum in the even sector shows a Dirac node like structure, which is suggested as an implication of gapless spinon excitations<sup>66</sup>. The different DMRG results in the two sectors reasonably imply that *either* the putative gapped spin liquid is not yet well developed as the strong finite-size effects in numerical calculation, *or* a gapless spin liquid is possible. In the variational study, a U(1) Dirac gapless spin liquid indeed possesses the best variational energy<sup>67</sup>. The nature of this spin liquid remains an open question. To shed more light on this spin liquid phase, the modified  $J_1 - J_2$  triangular models have been investigated<sup>72-75</sup>. Interestingly, the variational<sup>73</sup> and ED calculations<sup>74</sup> suggest a possible CSL at the neighbor of the  $J_1 - J_2$  spin liquid, which seems to be similar to the situation in the kagome model and deserves more studies. Besides, the quantum phase transition between the two spin liquid phases is also far from clear.

In this article, we study the spin-1/2  $J_1 - J_2$  Heisenberg model on the triangular lattice with additional time-reversal symmetry (TRS) breaking chiral interaction  $J_\chi$  using DMRG simulations. The model Hamiltonian is given as

$$H = J_1 \sum_{\langle i,j \rangle} \vec{S}_i \cdot \vec{S}_j + J_2 \sum_{\langle\langle i,j \rangle\rangle} \vec{S}_i \cdot \vec{S}_j + J_\chi \sum_{\Delta/\nabla} (\vec{S}_i \times \vec{S}_j) \cdot \vec{S}_k,$$

where  $J_1$  and  $J_2$  denote the NN and the NNN interactions, respectively. The scalar chiral interaction  $J_\chi$  has the same magnitude for all the up ( $\Delta$ ) and down ( $\nabla$ ) triangles, and the three sites  $i, j, k$  for  $J_\chi$  follow the clockwise order in all the triangles as shown in Fig. 1(a). Physically, the scalar chiral interaction  $J_\chi$  term can be induced in the Hubbard model with large  $U$  in a magnetic field<sup>76,77</sup>. Starting from the Hubbard model, a  $t/U$  ( $t$  and  $U$  are the hopping and interaction respectively) expansion to the second order at half filling gives the effective chiral interaction  $J_\chi(\vec{S}_i \times \vec{S}_j) \cdot \vec{S}_k$  with  $J_\chi \sim \Phi t^3/U^2$ , where  $\Phi$  is the magnetic flux enclosed by the triangle. We take  $J_1 = 1.0$  as the energy scale. Using DMRG simulation, we obtain a quantum phase diagram as shown in Fig. 1(d). Besides the  $120^\circ$  Néel phase, the stripe phase, and the time-reversal invariant spin liquid in the  $J_1 - J_2$  model (here we denote it as  $J_1 - J_2$  SL), we find a large regime of the non-coplanar tetrahedral order for large  $J_\chi$ , whose spin configuration is shown in Fig. 1(c). Below the tetrahedral phase for  $J_2 \lesssim 0.25$ , we identify a CSL as the  $\nu = 1/2$  bosonic fractional quantum Hall state by observing the gapless chiral edge mode. The strong nematic order of bond energy suggests a possible spontaneous lattice rotational symmetry breaking and implies an emergent nematic CSL. By studying the spin triplet gap and entanglement spectrum, we observe a transition from the  $J_1 - J_2$  SL to the CSL at small chiral interaction. While we find a large spin triplet gap above the overall ground state (in the odd sector) in the CSL phase, the small triplet gap in the even sector suggests that on our studied system size the topological nature in the even sector may not have been fully de-

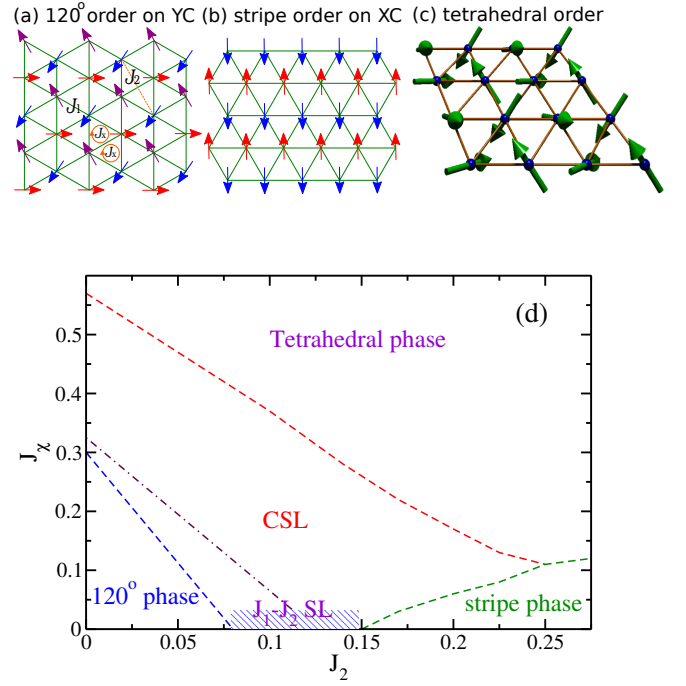


FIG. 1. Model Hamiltonian and quantum phase diagram of the spin-1/2  $J_1 - J_2 - J_\chi$  Heisenberg model on the triangular lattice. (a) and (b) are the schematic figures of the  $120^\circ$  and the stripe magnetic order on the XC and YC cylinders. The triangular model has the nearest-neighbor  $J_1$ , next-nearest-neighbor  $J_2$ , and three-spin scalar chiral interaction  $J_\chi$ . For all the triangles, the chiral interactions have the same chirality direction. (c) Tetrahedral magnetic order on the triangular lattice. This order has four sublattices with spins pointing toward the corners of a tetrahedron. (d) Quantum phase diagram of the model with growing  $J_2$  and  $J_\chi$ . The model shows the  $120^\circ$  magnetic order phase,  $J_1 - J_2$  spin liquid ( $J_1 - J_2$  SL) phase, stripe magnetic order phase, chiral spin liquid (CSL) phase, and tetrahedral phase. The phase boundaries (dashed lines) are obtained by measuring magnetic order parameter and spin correlation function. The dot-dashed line is the classical phase boundary between the  $120^\circ$  magnetic order and the tetrahedral order.

veloped. A possible reason is that this CSL regime generated by increasing  $J_\chi$  is near the phase boundaries from the CSL to the neighboring phases. In the  $J_1 - J_2$  triangular model, the triplet gap in the even sector seems to be vanished, which could be consistent with the larger correlation length found in DMRG calculation<sup>65,66</sup> and may suggest a possible gapless spin liquid<sup>67</sup>, which deserves more studies.

We study the system with cylinder geometry using DMRG<sup>78</sup> with spin rotational SU(2) symmetry<sup>79</sup>. We choose two geometries that have one lattice direction parallel to either the  $x$  axis (XC) or the  $y$  axis (YC), as shown in Figs. 1(a)-(b). These cylinders are denoted as XC(YC) $L_y$ - $L_x$ , where  $L_y$  and  $L_x$  are the numbers of site along the two directions. To study the phase diagram and characterize the CSL phase, we perform calculations on the systems with  $L_y$  up to 8 and 10. We keep up to 4000 SU(2) states to obtain accurate results with the truncation error less than  $10^{-5}$  in most calculations.

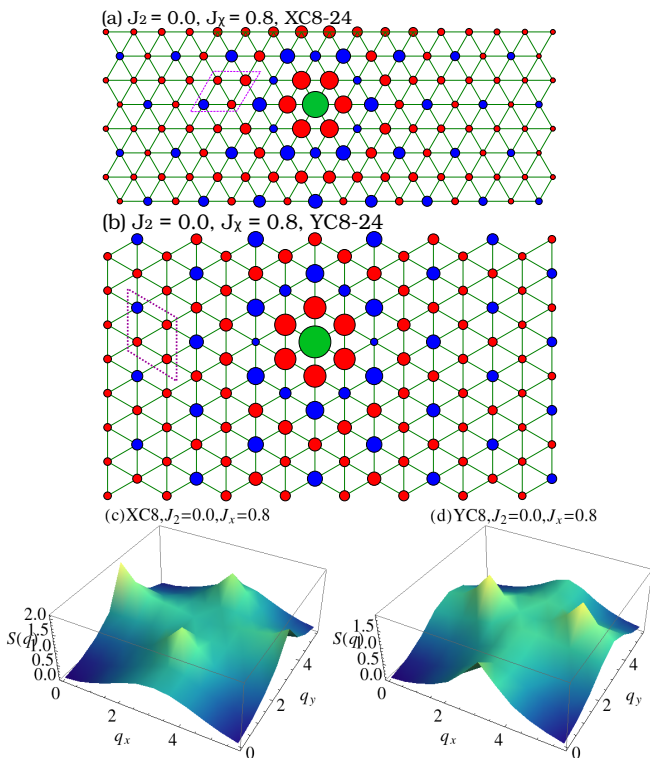


FIG. 2. Tetrahedral magnetic order for  $J_2 = 0.0$ ,  $J_\chi = 0.8$ . (a) and (b) are the spin correlation functions  $\langle \vec{S}_i \cdot \vec{S}_j \rangle$  in real space for the XC8-24 and YC8-24 cylinders, respectively. The green circle denotes the reference spin. The blue and red circles denote the positive and negative correlations, respectively. The magnitude of correlations are proportional to the square of circle area. The spin correlations on both geometries are consistent with the tetrahedral magnetic order with the unit cell shown by the dashed diamond. (c) and (d) are the corresponding spin structure factor  $S(\vec{q})$  of (a) and (b). On the XC and YC cylinders, the tetrahedral state has the structure factor peaks at  $\vec{q} = (0, \pi)$ ,  $(\pi, \pi/2)$  and  $(\pi/2, \pi)$ , respectively.

## II. TETRAHEDRAL ORDER AND $120^\circ$ ORDER

For  $J_2 = 0.0$ , the triangular model has a coplanar  $120^\circ$  magnetic order at  $J_\chi = 0.0$ <sup>46,47,80,81</sup>. In the large  $J_\chi$  limit, a classical spin analysis finds a tetrahedral magnetic state with the spins of the four sublattices pointing toward the corners of a tetrahedron<sup>82</sup> (see Fig. 1(b)). In the classical picture, the  $120^\circ$  ordered state has the energy per site  $E_{120} = -3J_1/2 + 3J_2$ , the stripe ordered state has the energy  $E_{\text{stripe}} = -J_1 - J_2$ , and the tetrahedral ordered state has the energy  $E_{\text{tetra}} = -J_1 - J_2 - 8\sqrt{3}J_\chi/9$ . Thus we can get a classical phase diagram in the  $J_2 - J_\chi$  plane. In Fig. 1(d), the dottashed line denotes the classical phase boundary between the  $120^\circ$  and the tetrahedral phase. For  $J_\chi = 0.0$ ,  $J_2 > 0.125$ , the stripe state and the tetrahedral state have the degenerate energy. By switching on the chiral interaction, the tetrahedral state immediately gets the lower energy. In quantum model, we first investigate whether this tetrahedral order could survive for the spin-1/2 system with strong quantum fluctuations. In Figs. 2(a)-(b), we demon-

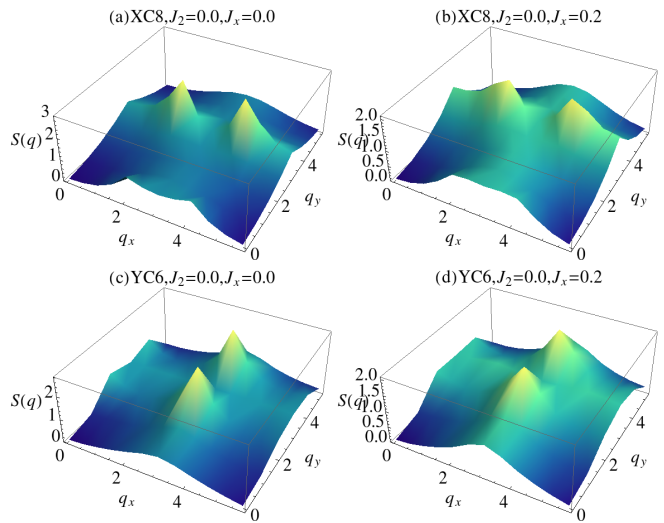


FIG. 3. Spin structure factor  $S(\vec{q})$  in the  $120^\circ$  magnetic order phase. (a) and (b) are obtained from the middle XC8-12 sites on the XC8-30 cylinder, and (c) and (d) are obtained from the middle YC6-12 sites on the YC6-30 cylinder. Both XC and YC systems exhibit the characteristic peak of the  $120^\circ$  order at  $\vec{q} = (2\pi/3, \pi)$  and  $(\pi, 2\pi/3)$ , respectively.

strate the spin correlations  $\langle \vec{S}_i \cdot \vec{S}_j \rangle$  for  $J_2 = 0.0$ ,  $J_\chi = 0.8$  on both the XC8-24 and YC8-24 cylinders. The dashed diamonds denote the unit cell of the spin correlation, which is consistent with the four sublattice structure of the tetrahedral order. The spin correlation functions decay quite slowly in both systems, indicating an established magnetic order. In Figs. 2(c)-(d), we show the corresponding spin structure factor  $S(\vec{q}) = \frac{1}{N} \sum_{i,j} \langle \vec{S}_i \cdot \vec{S}_j \rangle e^{i\vec{q} \cdot (\vec{r}_i - \vec{r}_j)}$  of the tetrahedral state on both cylinder geometries, which has the ordering peaks at  $\vec{q} = (0, \pi)$ ,  $(\pi, \pi/2)$  and  $(\pi/2, \pi)$  on the XC8 and YC8 cylinders, respectively.

For small  $J_\chi$  interaction we expect the  $120^\circ$  magnetic order. In Fig. 3, we show the spin structure factor for  $J_\chi = 0.0, 0.2$  on both the XC8 and YC6 cylinders. For a finite  $J_\chi = 0.2$ , the characteristic peak of the  $120^\circ$  order is still very stable, indicating the dominant three-sublattice spin structure.

## III. QUANTUM SPIN LIQUIDS

### A. Chiral spin liquid

For showing our results of the chiral spin liquid phase, we choose the parameters with fixed  $J_2 = 0.1$ , where the system is in the  $J_1 - J_2$  SL in the absence of the chiral interaction<sup>63-67</sup> (we have also studied other  $J_2$  such as  $J_2 = 0.125$ , which gives the same results). In our DMRG simulation of spin liquid phase on cylinder geometry, we control the even/odd parity of spinon flux in the ground state by removing or adding a spin-1/2 on each open edge of cylinder<sup>29,64,65</sup>.

We first exclude the conventional orders in the CSL phase. We show the spin correlations in Fig. 4(a), where the correla-

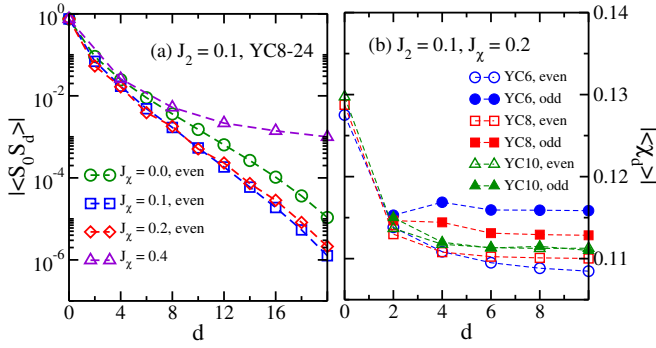


FIG. 4. Vanished magnetic order and non-zero chiral order in the CSL phase. (a) Log-linear plot of spin correlations for  $J_2 = 0.1$  and different  $J_x$  on the YC8-24 cylinder. (b) Distance dependence of the chiral order of triangle  $|\langle \chi_d \rangle|$  from the open boundary to the bulk of cylinder for  $J_2 = 0.1$ ,  $J_x = 0.2$  for different systems.

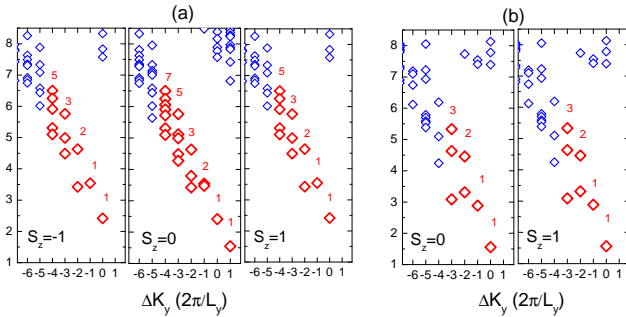


FIG. 5. Characterizing the CSL phase through the entanglement spectrum. Entanglement spectra of the ground states in the even (a) and odd (b) sectors for  $J_2 = 0.1$ ,  $J_x = 0.2$  on the  $L_y = 8$  cylinder.  $\lambda_i$  is the eigenvalue of the reduced density matrix obtained by bipartiting the cylinder system. The numbers denote the near degenerate pattern  $\{1, 1, 2, 3, 5, 7, \dots\}$  of the low-lying spectrum with different relative momentum quantum number  $\Delta k_y$  in each spin- $S_z$  sector.

tions in the CSL phase decay faster than those in the  $J_1 - J_2$  SL, indicating the vanished magnetic order. In Fig. 4(b), we plot the triangle chiral order  $\langle \chi_{\Delta_i} \rangle$  along the  $x$  direction of cylinder. Different from the decayed chiral order in the  $J_1 - J_2$  triangular model<sup>65,66</sup>, here it rapidly converges to finite value and seems to be robust with increasing system width. For  $L_y = 6, 8, 10$ , the chiral orders in both sectors approach to each other, which agrees with the consistent local orders in different sectors of gapped spin liquid. Similar to the  $J_1 - J_2$  SL<sup>64-66</sup>, lattice translational symmetry is also preserved in the CSL phase, which we do not discuss in detail but show an example in Fig. 7.

Next, we characterize the CSL by identifying the conformal field theory (CFT) that describes the gapless edge excitations through entanglement spectrum<sup>83</sup>. Since this strategy was proposed<sup>83</sup>, the ES has been shown as a powerful tool to identify different topological orders with edge states<sup>84,85</sup>. The nature of the CSLs in the kagome and honeycomb spin models have been characterized using ES<sup>14,16,22,23</sup>. In Fig. 5, we show the ES of the reduced density matrix for half the

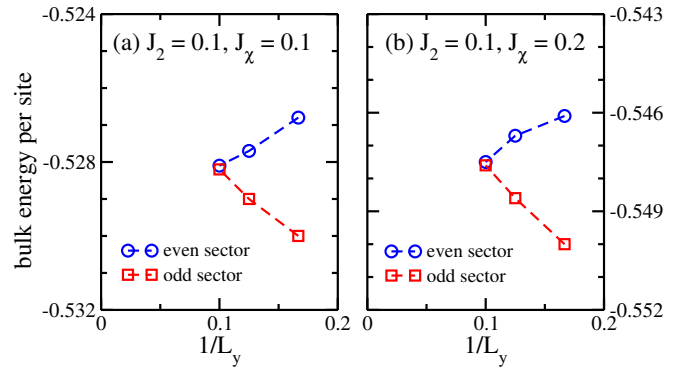


FIG. 6. Near-degenerate ground states in the CSL phase. Size dependence of the ground-state energy for  $J_2 = 0.1$ ,  $J_x = 0.1, 0.2$  in both the even and odd sectors on the YC6, YC8, and YC10 cylinders.

cylinder in both sectors. By tracing out half of the degrees of freedom for the density matrix by bipartiting the cylinder, we obtain the reduced density matrix and its eigenvalues  $\lambda_i$ . We focus on the leading eigenvalues by showing  $-\ln \lambda_i$  in Fig. 5. The spectra are labeled by the quantum number total spin  $S_z$  and relative momentum quantum number along the  $y$  direction  $\Delta k_y$ <sup>84,85</sup>. The leading spectra in both sectors have the degeneracy pattern  $\{1, 1, 2, 3, 5, 7, \dots\}$  with increasing  $\Delta k_y$  in each  $S_z$  sector, which follow the chiral  $SU(2)_1$  Wess-Zumino-Witten CFT theory of the  $\nu = 1/2$  fractional quantum Hall state<sup>86</sup>. The spectra of the even and odd sectors are symmetric about  $S_z = 0$  and  $1/2$  respectively, indicating a spin-1/2 at each end of cylinder in the odd (spinon) sector. The similar degeneracy pattern of entanglement spectra have also been found in the CSLs in the kagome and honeycomb spin models<sup>14,16,22,23</sup>. We further demonstrate the near-degenerate ground states in the CSL phase. In Fig. 6, we show the bulk energies in both the even and odd sectors, where the energy difference drops fast with increasing  $L_y$ . For  $L_y = 10$ , the energy difference is vanishing small, in consistent with the near-degenerate ground states in the two sectors.

For the  $J_1 - J_2$  SL, DMRG calculations find the large lattice nematic order in the odd sector (defined as the energy difference between the zigzag and vertical bonds)<sup>64-66</sup>, suggesting a spin liquid with possible spontaneous rotational symmetry breaking. However, the nematic order in the even sector exhibits the opposite nematic pattern from the odd sector, which seems to approach vanishing with increasing  $L_y = 6, 8, 10$ <sup>64-66</sup>. In the CSL phase, we also calculate the NN bond energy  $\langle \vec{S}_i \cdot \vec{S}_j \rangle$  on the YC cylinder as shown in Figs. 7(a)-(b). On the YC8 cylinder, we also find the strong bond energy anisotropy and the nematic patterns are different in the two sectors. For studying the nematic order, we show the nematic order on different cylinders in Fig. 7(c) with a comparison to the data for  $J_x = 0.0$ <sup>64-66</sup>. For  $L_y = 6, 8, 10$ , while the nematic order in the odd sector keeps growing with  $L_y$ ; in the even sector it also appears to approach zero. The overall behaviors of the nematic order in the CSL are consistent with those in the  $J_1 - J_2$  SL. We notice that the nematicity for the even sector in Fig. 7(c) shows a tendency to become

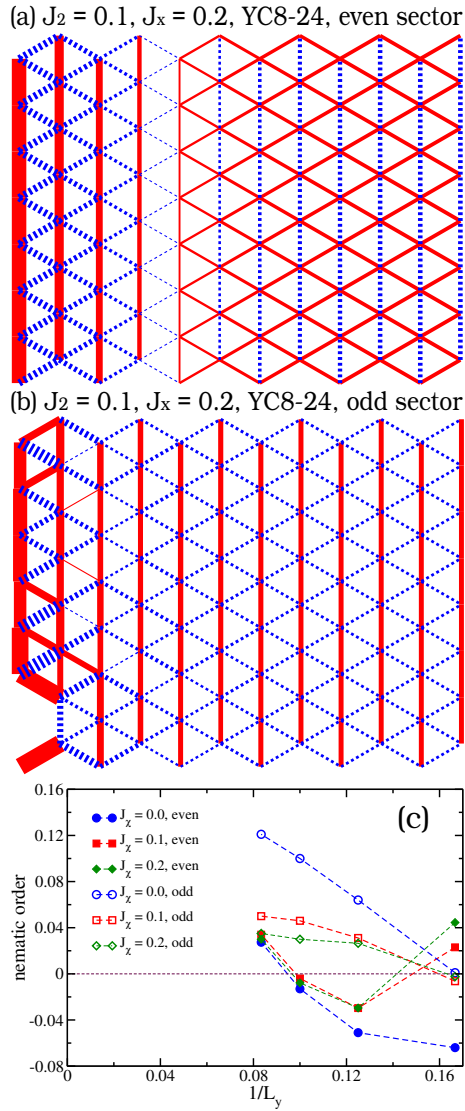


FIG. 7. Strong bond nematicity in the CSL phase. (a) and (b) are the nearest-neighbor bond energy  $\langle \vec{S}_i \cdot \vec{S}_j \rangle$  for  $J_2 = 0.1$ ,  $J_x = 0.2$  on the YC8-24 cylinder in the even and odd sectors. The left half systems are shown here. The odd sector in (b) is obtained by removing one site in each boundary of cylinder. In both figures, all the bond energy have subtracted a constant. The red solid and blue dashed bonds denote the negative and positive bond energies after subtraction. (c) Cylinder width dependence of bond nematic order for  $J_2 = 0.1$  in both the even and odd sectors on the YC ( $L_y = 6, 8, 10, 12$ ) cylinder. The nematic order is defined as the difference between the zigzag and the vertical bond energy. The data for  $J_x = 0.0$  at  $L_y = 6, 8, 10$  have been shown in Ref. 65.

positive with growing  $L_y$ . To shed more light on the nature of the nematicity, we calculate the bond energy for  $L_y = 12$  by keeping the SU(2) states up to 6000. We find that while the nematic order in the odd sector shows a consistent behavior, the order in the even sector changes the pattern to that of the odd sector on the YC12 cylinder. Our results imply that in both the  $J_1 - J_2$  SL and the CSL, the even sector may also host a nematic order in large size, suggesting possible nematic

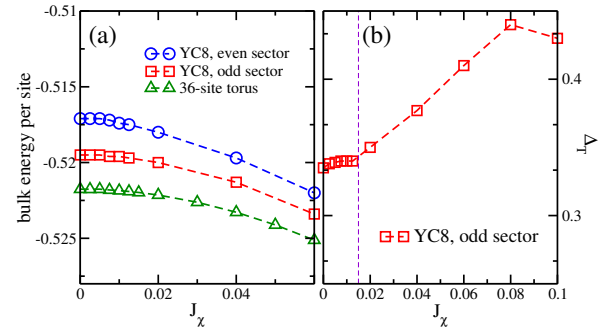


FIG. 8. Ground-state energy (a) and spin triplet gap  $\Delta_T$  (b) versus  $J_x$  for  $J_2 = 0.1$ . The spin triplet gap is obtained by sweeping the middle  $8 \times 16$  sites in the total spin  $S = 1$  sector based on the ground state with the lowest energy in the odd sector.

spin liquids. While CSL has been discovered in several spin models, the nematic CSL with coexisting topological order and nematic order has not been reported in a microscopic spin model as far as we know. In a strong-coupling perspective, a nematic FQH may be viewed as a partially melted solid, where the nematic FQH is proximate to the phase with broken translational and rotational symmetries<sup>87</sup>. If the translational order is melted by tuning external parameter but nematic order is preserved, a nematic FQH might be obtained. Here, the CSL in the triangular model emerges at the neighbor of a stripe phase, which breaks translational and rotational symmetries. The possible nematicity of the CSL might be understood as a partially melted stripe order.

## B. Transition between the two spin liquids

Now we study the quantum phase transition from the  $J_1 - J_2$  SL to the CSL. We choose  $J_2 = 0.1$  and switch on the chiral interaction  $J_x$ . In Fig. 8(a), we show the ground-state energy on the YC8 cylinder as well as on the  $6 \times 6$  torus. The energy varies smoothly with growing  $J_x$ , and we notice the slight change of energy for  $J_x \lesssim 0.02$ . Then we compute the spin triplet gap  $\Delta_T$  on the YC8 cylinder based on the ground state with the lowest energy, which is in the odd sector as shown in Fig. 6. The triplet gap is obtained by sweeping the total spin-1 sector in the bulk of long cylinder<sup>29</sup>. We compare the obtained spin triplet gap by sweeping the spin-1 sector on the different system lengths, and we find the well converged triplet gap (one example can be found as the red square in Fig. 11(c)). In Fig. 8(b), we show the gap obtained by sweeping the middle  $8 \times 16$  sites in the spin-1 sector based on the ground state in the odd sector on the YC8-24 cylinder. The triplet gap changes slightly for  $J_x \lesssim 0.02$ . Above  $J_x \simeq 0.02$ , the gap grows fast, consistent with the non-zero gap in the CSL phase. The  $J_x$  dependence of energy and triplet gap imply a possible phase transition at small  $J_x$ .

Next, we study the entanglement spectrum. As shown in Figs. 9(a)-(b) for  $J_x = 0.01, 0.02$  in the odd sector with total spin  $S^z = 0$ , the ES exhibit some features of the ES

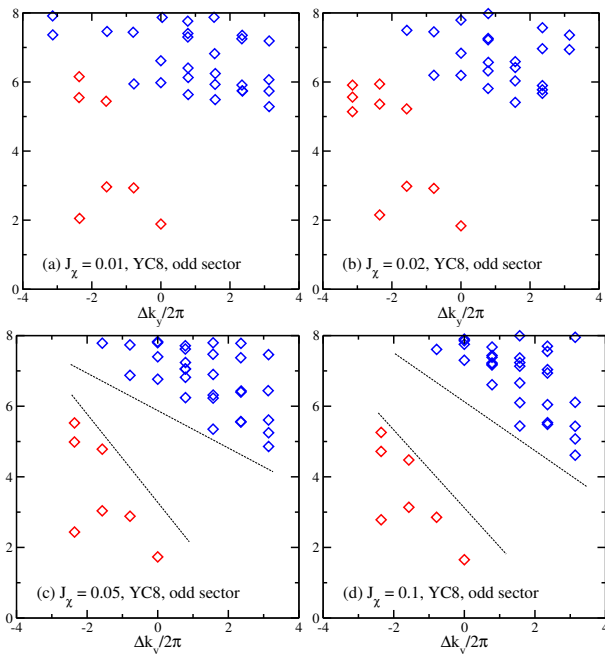


FIG. 9. Entanglement spectra of the ground state in the odd sector for  $J_2 = 0.1$  and different  $J_\chi$  on the YC8-24 cylinder.  $\Delta k_y$  is the relative momentum quantum number along the  $y$  direction.  $y$  label denotes the eigenvalue of the reduced density matrix  $-\ln \lambda_i$ . Here we show the spectra for total spin  $S^z = 0$  sector.

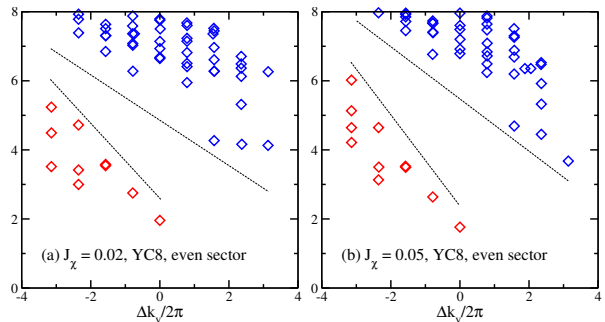


FIG. 10. Entanglement spectra of the ground state in the even sector for  $J_2 = 0.1$  and different  $J_\chi$  on the YC8-24 cylinder. The labels are the same as Fig. 9.

for  $J_\chi = 0.066$ , where four eigenvalues are found below the higher spectrum. We also notice that with increasing  $J_\chi$ , some eigenvalues in the higher spectrum are decreasing gradually as marked by red in Figs. 9(a)-(b). For  $J_\chi = 0.05, 0.1$  as shown in Figs. 9(c)-(d), the decreasing eigenvalues seem to merge with the low-lying levels, which are separated by an ES gap from the higher spectrum. The ES levels below the gap exhibit the near degenerate pattern  $\{1, 1, 2, 3\}$ , which is consistent with the Laughlin CSL. The entanglement spectrum also suggests a phase transition at small  $J_\chi$ , which agrees with the transition suggested by energy and triplet gap in Fig. 8. In the even sector for  $J_\chi = 0.0$ , the low-lying part of the ES shows a deformed two-spinon continuum structure<sup>66</sup>. By switching on the chiral interaction, the low-lying part of the ES quickly

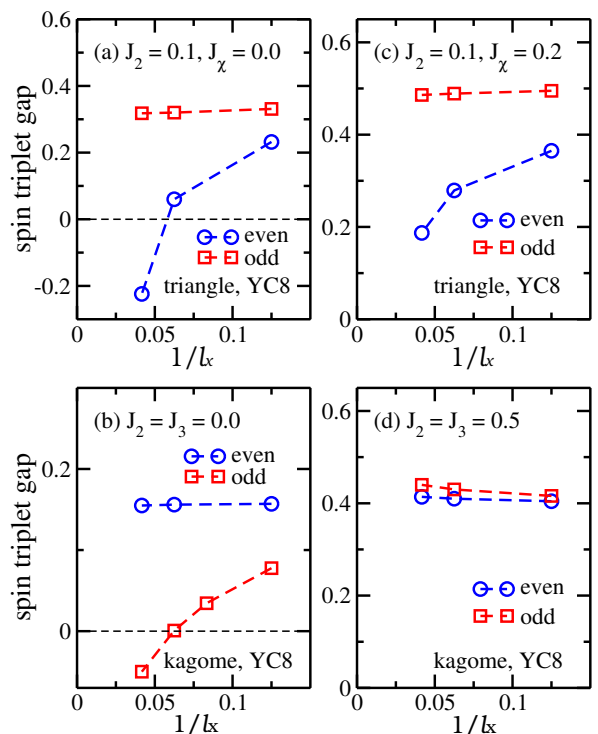


FIG. 11. Spin triplet gap versus cylinder length  $l_x$  in the triangular and kagome models. We obtain the spin triplet gap by calculating the ground state on long cylinder first and then sweeping the bulk sites for the ground state in spin quantum number  $S = 1$  sector for a given length  $l_x$ . (a) and (c) are the  $1/l_x$  dependence of the gap on the YC8 cylinder in the  $J_1 - J_2$  SL ( $J_2 = 0.1, J_\chi = 0.0$ ) and CSL ( $J_2 = 0.1, J_\chi = 0.2$ ) for the triangular model. (b) and (d) are the  $1/l_x$  dependence of the gap on the YC8 cylinder in the kagome spin liquid ( $J_2 = J_3 = 0.0$ ) and CSL ( $J_2 = J_3 = 0.5$ ) for the kagome model.

changes to the structure that looks like the one in the CSL, which are shown in Fig. 10 and may suggest a stronger tendency to the chiral state in the even sector.

We also compute the spin triplet gap. For a comparison, we demonstrate the results of the same calculation for the spin-1/2  $J_1 - J_2 - J_3$  kagome model. Here, we obtain the triplet gap by calculating the ground state on long cylinder first (for example YC8-40) and then sweeping the bulk sites in the total spin  $S = 1$  sector for the given bulk length  $l_x$ <sup>29</sup>. For the  $J_1 - J_2$  triangular model shown in Fig. 11(a), the spin gap measured from the overall ground state (in the odd sector) is robust with increasing  $l_x$ . However, the gap measured from the ground state in the even sector decreases with  $l_x$ . On large  $l_x$ , the ground state in the even sector has the higher energy than the obtained state in the spin-1 sector, which suggests that the triplet gap is lower than the total energy difference between the two sectors and is unlikely to support a well established gapped spin liquid. For the  $J_1$  kagome model ( $J_2 = J_3 = 0.0$ ) as shown in Fig. 11(b) on the YC8 cylinder, while the triplet gap measured from the overall ground state (in the even sector for the kagome spin liquid) is quite robust (consistent with the previous result<sup>29,30</sup>), the gap in the odd

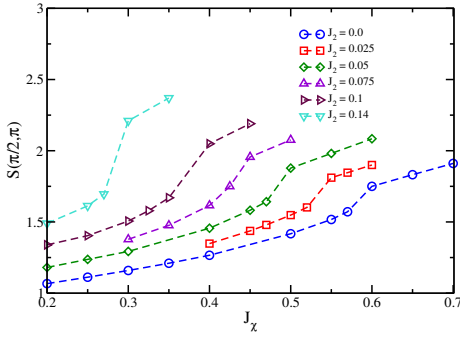


FIG. 12.  $J_\chi$  dependence of the tetrahedral magnetic structure factor  $S(\pi/2, \pi)$  on the YC8 cylinder for different  $J_2$  couplings. The structure factor is obtained from the Fourier transform of the spin correlations of the middle  $8 \times 12$  sites on the YC8-24 cylinder. With increasing  $J_\chi$ , tetrahedral order shows a sharp increase that characterizes the phase transition to the tetrahedral phase.

sector decreases fast with  $l_x$  and tends to vanish, seemingly similar to the behaviors found in Fig. 11(a).

In the CSL phase as shown in Fig. 11(c), the overall triplet gap is also robust; but the gap in the even sector still decreases with  $l_x$ . In the well established CSL phase, for example the CSL phase in the kagome model as shown in Fig. 11(d)<sup>15</sup>, one can find the robust triplet gap in both sectors. The decreasing gap of the triangular CSL in the even sector suggests that on our studied system size the topological nature in the even sector is not fully developed. A possible reason is that this CSL regime is very close to the phase boundaries from the CSL to the neighboring phases.

#### IV. QUANTUM PHASE DIAGRAM

First of all, we study the phase transition from the tetrahedral phase to the CSL phase by calculating magnetic structure factor. In Fig. 12, we show the  $J_\chi$  dependence of the tetrahedral structure factor peak on the YC8 cylinder, which is at  $\vec{q} = (\pi/2, \pi)$ . With increasing  $J_\chi$ ,  $S(\pi/2, \pi)$  shows a jump that characterizes the phase transition. Above the transition  $J_\chi$ , we find that the spin correlations decay quite slowly, consistent with a magnetic order developed. On the smaller YC6 and XC8 cylinders, the tetrahedral structure factor peak appears to increase smoothly, which may be owing to the finite-size effects. We show the phase boundary in Fig. 1 based on the results on the larger YC8 cylinder.

By increasing the chiral interaction  $J_\chi$  in the  $120^\circ$  phase for  $J_2 \lesssim 0.08$ , the magnetic order is suppressed, leading to a transition from the magnetic order to the non-magnetic spin liquid phase. On our studied system size, we do not find sharp features to characterize this transition. Thus we estimate a qualitative phase boundary as shown in Fig. 1(c) by comparing spin correlation function and magnitude of spin structure factor on the YC8 cylinder with the results at  $J_2 = 0.08$ ,  $J_\chi = 0$ , where the system has the transition from the  $120^\circ$  phase to the  $J_1 - J_2$  SL phase. We roughly take the parameter points which have the similar magnitudes of spin correlations and spin

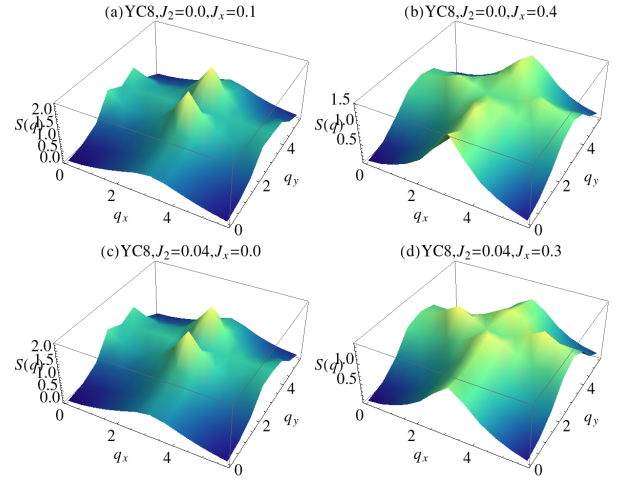


FIG. 13. Spin structure factor  $S(\vec{q})$  in the  $120^\circ$  magnetic order phase and the non-magnetic CSL phase. The structure factor is obtained from the middle  $8 \times 12$  sites on the YC8-24 cylinder. In the ordered phase for (a) and (c),  $S(\vec{q})$  has the peak at  $\vec{q} = (\pi, 2\pi/3)$ . In the CSL phase for (b) and (d),  $S(\vec{q})$  is featureless.

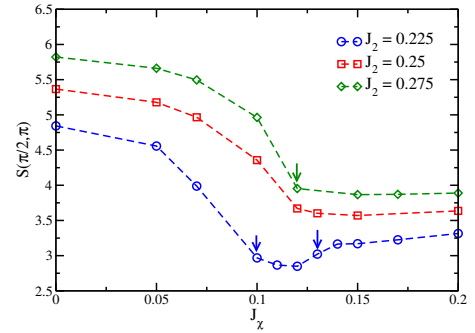


FIG. 14.  $J_\chi$  coupling dependence of the magnetic structure factor at the momentum  $\vec{q} = (\pi/2, \pi)$  for  $J_2 = 0.225, 0.25, 0.275$  on the YC8-24 cylinder. The structure factor is obtained from the spin correlations of the middle  $8 \times 12$  sites. The arrows denote the phase transitions. For  $J_2 = 0.225$ , we find two transitions with a CSL phase in between. For  $J_2 = 0.25$  and  $0.275$ , we find a direct phase transition from the stripe phase to the tetrahedral phase.

structure factor compared with those at  $J_2 = 0.08$ ,  $J_\chi = 0$  as the phase boundary. In Fig. 13, we show the spin structure factor  $S(\vec{q})$ , which characterizes the present and absent magnetic order in the two phases.

As shown in Fig. 1(c), the stripe phase goes to the tetrahedral phase with or without an intermediate CSL phase depending on  $J_2$ . We calculate the spin correlations and structure factor on the YC8 cylinder. In both the stripe and the tetrahedral phase, spin structure factor shows the peak at  $\vec{q} = (\pi/2, \pi)$ . For the case with the intermediate CSL phase, we find that  $S(\pi/2, \pi)$  first decreases with growing  $J_\chi$  and then keeps small in the CSL phase; with further increasing  $J_\chi$ ,  $S(\pi/2, \pi)$  shows a jump at the transition to the tetrahedral phase, which is shown for  $J_2 = 0.225$  in Fig. 14. On the other hand, for  $J_2 \gtrsim 0.25$ ,  $S(\pi/2, \pi)$  decreases fast with  $J_\chi$  in the stripe

phase and changes slowly in the tetrahedral phase, showing a kink to characterize the phase transition. We remark that on the smaller YC6 cylinder for the  $J_1 - J_2$  model, the magnetic order is weak at  $0.15 \lesssim J_2 \lesssim 0.2$ ; however, on the larger YC and XC cylinders the stripe order is quite robust. We demonstrate our phase diagram based on the large-size results.

## V. SUMMARY AND DISCUSSION

We have studied the competing quantum phases of the spin-1/2 triangular  $J_1 - J_2$  Heisenberg model with the additional scalar chiral interaction  $J_\chi$  for  $0 \leq J_2 \leq 0.3$  and  $0 \leq J_\chi \leq 1.0$  by DMRG simulations. As shown in Fig. 1(c), we find five phases: a non-coplanar tetrahedral magnetic order phase, a  $120^\circ$  order phase, a stripe order phase, a  $J_1 - J_2$  SL phase, and a chiral spin liquid (CSL) phase. The CSL is identified as the  $\nu = 1/2$  bosonic fractional quantum Hall state, which seems to arise as a result of quantum fluctuations around the phase boundaries of the classical magnetic orders. In particular, the CSL state exhibits a strong bond anisotropy, strongly suggesting a nematic CSL with coexisting topological order and nematic order. We argue that the nematicity can be understood as a partially melted stripe order. The emergent CSL induced from quantum fluctuations around classical phase boundaries has also been found in the kagome<sup>21,23,42</sup> and honeycomb<sup>22</sup> models, which may represent a common mechanism to generate novel quantum phases from frustration. We remark that while the analytic analyses suggest that the CSL is unlikely to emerge in the triangular model built out of weakly coupled chains with chiral interaction<sup>19</sup>, DMRG results indicate that the CSL can emerge in the strong coupling regime.

By measuring the spin triplet gap and entanglement spectrum on the YC8 cylinder, we find a transition from the  $J_1 - J_2$  SL to the CSL at small chiral coupling. We also

compute the spin triplet gap on cylinder geometry. While the gap above the overall ground state (in the odd sector) is robust, the one in the even sector seems to be small in both spin liquid phases. In the CSL phase, the small gap suggests that the even sector may be not well developed on our studied system sizes. To find a robust CSL in finite-size calculation, other interactions may be needed besides the chiral interaction. In the  $J_1 - J_2$  SL, the vanishing gap in the even sector also indicates that for a gapped spin liquid scenario the even sector is not well established. On the other hand, in the gapless spin liquid scenario<sup>67</sup>, one finds it inconsistent with the odd sector exhibiting a large gap based on DMRG calculations ( $\Delta_T \simeq 0.35J_1$  on the YC8 cylinder and the size scaling seems to suggest a large gap in the large-size limit<sup>64,65</sup>). However, the spin gap measured in DMRG calculations may also have large finite-size effects, which requires further investigations. We hope that future studies will be able to resolve between these scenarios more clearly.

This research is supported by the state of Florida (S.S.G.), National Science Foundation Grants DMR-1157490 (S.S.G. and K.Y.), DMR-1442366 (K.Y.), and DMR-1408560 (D.N.S.). Work at Los Alamos was supported by U.S. DOE National Nuclear Security Administration through Los Alamos National Laboratory LDRD Program (W.Z. and J.-X.Z.), and in part supported by the Center for Integrated Nanotechnologies, a U.S. DOE Basic Energy Sciences user facility.

*Note Added.*— While completing this work, we became aware of a related paper<sup>88</sup> that also studies the robustness of the  $J_1 - J_2$  spin liquid against the chiral interaction in the same  $J_1 - J_2 - J_\chi$  triangular model. We find the overall agreement with Ref. 88.

- 
- <sup>1</sup> Lucile Savary and Leon Balents, “Quantum spin liquids: a review,” *Reports on Progress in Physics* **80**, 016502 (2016).
  - <sup>2</sup> Patrick A. Lee, Naoto Nagaosa, and Xiao-Gang Wen, “Doping a mott insulator: Physics of high-temperature superconductivity,” *Rev. Mod. Phys.* **78**, 17–85 (2006).
  - <sup>3</sup> Daniel S. Rokhsar and Steven A. Kivelson, “Superconductivity and the quantum hard-core dimer gas,” *Phys. Rev. Lett.* **61**, 2376–2379 (1988).
  - <sup>4</sup> G. Baskaran, “Novel local symmetries and chiral-symmetry-broken phases in  $s=1/2$  triangular-lattice heisenberg model,” *Phys. Rev. Lett.* **63**, 2524–2527 (1989).
  - <sup>5</sup> N. Read and Subir Sachdev, “Large- $n$  expansion for frustrated quantum antiferromagnets,” *Phys. Rev. Lett.* **66**, 1773–1776 (1991).
  - <sup>6</sup> Subir Sachdev, “Kagome and triangular-lattice heisenberg antiferromagnets: Ordering from quantum fluctuations and quantum-disordered ground states with unconfined bosonic spinons,” *Phys. Rev. B* **45**, 12377–12396 (1992).
  - <sup>7</sup> Kun Yang, L. K. Warman, and S. M. Girvin, “Possible spin-liquid states on the triangular and kagomé lattices,” *Phys. Rev. Lett.* **70**,

2641–2644 (1993).

- <sup>8</sup> L. Balents, M. P. A. Fisher, and S. M. Girvin, “Fractionalization in an easy-axis kagome antiferromagnet,” *Phys. Rev. B* **65**, 224412 (2002).
- <sup>9</sup> Hong Yao and Steven A. Kivelson, “Exact chiral spin liquid with non-abelian anyons,” *Phys. Rev. Lett.* **99**, 247203 (2007).
- <sup>10</sup> A. Kitaev, “Anyons in an exactly solved model and beyond,” *Annals of Physics* **321**, 2–111 (2006).
- <sup>11</sup> Darrell F. Schroeter, Eliot Kapit, Ronny Thomale, and Martin Greiter, “Spin hamiltonian for which the chiral spin liquid is the exact ground state,” *Phys. Rev. Lett.* **99**, 097202 (2007).
- <sup>12</sup> Ronny Thomale, Eliot Kapit, Darrell F. Schroeter, and Martin Greiter, “Parent hamiltonian for the chiral spin liquid,” *Phys. Rev. B* **80**, 104406 (2009).
- <sup>13</sup> Anne E. B. Nielsen, J. Ignacio Cirac, and Germán Sierra, “Laughlin spin-liquid states on lattices obtained from conformal field theory,” *Phys. Rev. Lett.* **108**, 257206 (2012).
- <sup>14</sup> B. Bauer, L. Cincio, B. P. Keller, M. Dolfi, G. Vidal, S. Trebst, and A. W. Ludwig, “Chiral spin liquid and emergent anyons in a Kagome lattice Mott insulator,” *Nature Communications* **5**,

- 5137 (2014).
- 15 Shou-Shu Gong, Wei Zhu, and DN Sheng, “Emergent chiral spin liquid: fractional quantum hall effect in a kagome heisenberg model,” *Scientific reports* **4**, 6317 (2014).
  - 16 Yin-Chen He, D. N. Sheng, and Yan Chen, “Chiral spin liquid in a frustrated anisotropic kagome heisenberg model,” *Phys. Rev. Lett.* **112**, 137202 (2014).
  - 17 Wen-Jun Hu, Wei Zhu, Yi Zhang, Shoushu Gong, Federico Becca, and D. N. Sheng, “Variational monte carlo study of a chiral spin liquid in the extended heisenberg model on the kagome lattice,” *Phys. Rev. B* **91**, 041124 (2015).
  - 18 Tobias Meng, Titus Neupert, Martin Greiter, and Ronny Thomale, “Coupled-wire construction of chiral spin liquids,” *Phys. Rev. B* **91**, 241106 (2015).
  - 19 Gregory Gorohovsky, Rodrigo G. Pereira, and Eran Sela, “Chiral spin liquids in arrays of spin chains,” *Phys. Rev. B* **91**, 245139 (2015).
  - 20 Krishna Kumar, Kai Sun, and Eduardo Fradkin, “Chiral spin liquids on the kagome lattice,” *Phys. Rev. B* **92**, 094433 (2015).
  - 21 Alexander Wietek, Antoine Sterdyniak, and Andreas M. Läuchli, “Nature of chiral spin liquids on the kagome lattice,” *Phys. Rev. B* **92**, 125122 (2015).
  - 22 Ciarán Hickey, Lukasz Cincio, Zlatko Papić, and Arun Paramekanti, “Haldane-hubbard mott insulator: From tetrahedral spin crystal to chiral spin liquid,” *Phys. Rev. Lett.* **116**, 137202 (2016).
  - 23 W. Zhu, S. S. Gong, and D. N. Sheng, “Interaction-driven fractional quantum hall state of hard-core bosons on kagome lattice at one-third filling,” *Phys. Rev. B* **94**, 035129 (2016).
  - 24 P. Mendels, F. Bert, M. A. de Vries, A. Olariu, A. Harrison, F. Duc, J. C. Trombe, J. S. Lord, A. Amato, and C. Baines, “Quantum magnetism in the paratacamite family: Towards an ideal kagomé lattice,” *Phys. Rev. Lett.* **98**, 077204 (2007).
  - 25 J. S. Helton, K. Matan, M. P. Shores, E. A. Nytko, B. M. Bartlett, Y. Yoshida, Y. Takano, A. Suslov, Y. Qiu, J.-H. Chung, D. G. Nocera, and Y. S. Lee, “Spin dynamics of the spin-1/2 kagome lattice antiferromagnet  $\text{ZnCu}_3(\text{OH})_6\text{Cl}_2$ ,” *Phys. Rev. Lett.* **98**, 107204 (2007).
  - 26 T.-H. Han, J. S. Helton, S. Chu, D. G. Nocera, J. A. Rodriguez-Rivera, C. Broholm, and Y. S. Lee, “Fractionalized excitations in the spin-liquid state of a kagome-lattice antiferromagnet,” *Nature (London)* **492**, 406–410 (2012).
  - 27 M. Fu, T. Imai, T.-H. Han, and Y. S. Lee, “Evidence for a gapped spin-liquid ground state in a kagome Heisenberg antiferromagnet,” *Science* **350**, 655–658 (2015).
  - 28 M. R. Norman, “Colloquium:herbertsmithite and the search for the quantum spin liquid,” *Rev. Mod. Phys.* **88**, 041002 (2016).
  - 29 S. Yan, D. A. Huse, and S. R. White, “Spin-Liquid Ground State of the  $S = 1/2$  Kagome Heisenberg Antiferromagnet,” *Science* **332**, 1173 (2011).
  - 30 Stefan Depenbrock, Ian P. McCulloch, and Ulrich Schollwöck, “Nature of the spin-liquid ground state of the  $s = 1/2$  heisenberg model on the kagome lattice,” *Phys. Rev. Lett.* **109**, 067201 (2012).
  - 31 Hong-Chen Jiang, Zhenghan Wang, and Leon Balents, “Identifying topological order by entanglement entropy,” *Nature Physics* **8**, 902–905 (2012).
  - 32 Jia-Wei Mei, Ji-Yao Chen, Huan He, and Xiao-Gang Wen, “Gapped spin liquid with  $F_2$  topological order for the kagome heisenberg model,” *Phys. Rev. B* **95**, 235107 (2017).
  - 33 C Waldtmann, H-U Everts, B Bernu, C Lhuillier, P Sindzingre, P Lecheminant, and L Pierre, “First excitations of the spin 1/2 heisenberg antiferromagnet on the kagomé lattice,” *The European Physical Journal B-Condensed Matter and Complex Systems* **2**, 501–507 (1998).
  - 34 A. M. Läuchli, J. Sudan, and R. Moessner, “The  $S = 1/2$  Kagome Heisenberg Antiferromagnet Revisited,” ArXiv e-prints (2016), [arXiv:1611.06990 \[cond-mat.str-el\]](https://arxiv.org/abs/1611.06990).
  - 35 Ying Ran, Michael Hermele, Patrick A. Lee, and Xiao-Gang Wen, “Projected-wave-function study of the spin-1/2 heisenberg model on the kagomé lattice,” *Phys. Rev. Lett.* **98**, 117205 (2007).
  - 36 Yasir Iqbal, Federico Becca, Sandro Sorella, and Didier Poilblanc, “Gapless spin-liquid phase in the kagome spin- $\frac{1}{2}$  heisenberg antiferromagnet,” *Phys. Rev. B* **87**, 060405 (2013).
  - 37 Yasir Iqbal, Didier Poilblanc, and Federico Becca, “Vanishing spin gap in a competing spin-liquid phase in the kagome heisenberg antiferromagnet,” *Phys. Rev. B* **89**, 020407 (2014).
  - 38 S. Jiang, P. Kim, J. H. Han, and Y. Ran, “Competing Spin Liquid Phases in the  $S = \frac{1}{2}$  Heisenberg Model on the Kagome Lattice,” ArXiv e-prints (2016), [arXiv:1610.02024 \[cond-mat.str-el\]](https://arxiv.org/abs/1610.02024).
  - 39 H. J. Liao, Z. Y. Xie, J. Chen, Z. Y. Liu, H. D. Xie, R. Z. Huang, B. Normand, and T. Xiang, “Gapless spin-liquid ground state in the  $s = 1/2$  kagome antiferromagnet,” *Phys. Rev. Lett.* **118**, 137202 (2017).
  - 40 Y.-C. He, M. P. Zaletel, M. Oshikawa, and F. Pollmann, “Signatures of Dirac cones in a DMRG study of the Kagome Heisenberg model,” ArXiv e-prints (2016), [arXiv:1611.06238 \[cond-mat.str-el\]](https://arxiv.org/abs/1611.06238).
  - 41 Laura Messio, Bernard Bernu, and Claire Lhuillier, “Kagome antiferromagnet: A chiral topological spin liquid?” *Phys. Rev. Lett.* **108**, 207204 (2012).
  - 42 Shou-Shu Gong, Wei Zhu, Leon Balents, and D. N. Sheng, “Global phase diagram of competing ordered and quantum spin-liquid phases on the kagome lattice,” *Phys. Rev. B* **91**, 075112 (2015).
  - 43 Yasir Iqbal, Didier Poilblanc, and Federico Becca, “Spin- $\frac{1}{2}$  heisenberg  $J_1$ - $J_2$  antiferromagnet on the kagome lattice,” *Phys. Rev. B* **91**, 020402 (2015).
  - 44 V. Kalmeyer and R. B. Laughlin, “Equivalence of the resonating-valence-bond and fractional quantum hall states,” *Phys. Rev. Lett.* **59**, 2095–2098 (1987).
  - 45 X. G. Wen, Frank Wilczek, and A. Zee, “Chiral spin states and superconductivity,” *Phys. Rev. B* **39**, 11413–11423 (1989).
  - 46 B. Bernu, C. Lhuillier, and L. Pierre, “Signature of néel order in exact spectra of quantum antiferromagnets on finite lattices,” *Phys. Rev. Lett.* **69**, 2590–2593 (1992).
  - 47 Luca Capriotti, Adolfo E. Trumper, and Sandro Sorella, “Long-range néel order in the triangular heisenberg model,” *Phys. Rev. Lett.* **82**, 3899–3902 (1999).
  - 48 Y. Shimizu, K. Miyagawa, K. Kanoda, M. Maesato, and G. Saito, “Spin liquid state in an organic mott insulator with a triangular lattice,” *Phys. Rev. Lett.* **91**, 107001 (2003).
  - 49 Y. Kurosaki, Y. Shimizu, K. Miyagawa, K. Kanoda, and G. Saito, “Mott transition from a spin liquid to a fermi liquid in the spin-frustrated organic conductor  $\kappa$ -(et) $_2$ cu $_2$ (cn) $_3$ ,” *Phys. Rev. Lett.* **95**, 177001 (2005).
  - 50 Satoshi Yamashita, Yasuhiro Nakazawa, Masaharu Oguni, Yugo Oshima, Hiroyuki Nojiri, Yasuhiro Shimizu, Kazuya Miyagawa, and Kazushi Kanoda, “Thermodynamic properties of a spin-1/2 spin-liquid state in a  $\kappa$ -type organic salt,” *Nature Physics* **4**, 459–462 (2008).
  - 51 Minoru Yamashita, Norihito Nakata, Yuichi Kasahara, Takahiko Sasaki, Naoki Yoneyama, Norio Kobayashi, Satoshi Fujimoto, Takasada Shibauchi, and Yuji Matsuda, “Thermal-transport measurements in a quantum spin-liquid state of the frustrated triangular magnet-(bedt-ttf) 2cu2 (cn) 3,” *Nature Physics* **5**, 44–47 (2009).
  - 52 Minoru Yamashita, Norihito Nakata, Yoshinori Senshu, Masaki

- Nagata, Hiroshi M Yamamoto, Reizo Kato, Takasada Shibauchi, and Yuji Matsuda, “Highly mobile gapless excitations in a two-dimensional candidate quantum spin liquid,” *Science* **328**, 1246–1248 (2010).
- <sup>53</sup> G. Misguich, C. Lhuillier, B. Bernu, and C. Waldtmann, “Spin-liquid phase of the multiple-spin exchange hamiltonian on the triangular lattice,” *Phys. Rev. B* **60**, 1064–1074 (1999).
- <sup>54</sup> Olexei I. Motrunich, “Variational study of triangular lattice spin-1/2 model with ring exchanges and spin liquid state in  $\kappa$ -( $\text{et}$ )<sub>2</sub> $\text{Cu}_2$ ( $\text{cn}$ )<sub>3</sub>,” *Phys. Rev. B* **72**, 045105 (2005).
- <sup>55</sup> D. N. Sheng, Olexei I. Motrunich, and Matthew P. A. Fisher, “Spin bose-metal phase in a spin- $\frac{1}{2}$  model with ring exchange on a two-leg triangular strip,” *Phys. Rev. B* **79**, 205112 (2009).
- <sup>56</sup> Ryan V. Mishmash, James R. Garrison, Samuel Bieri, and Cenke Xu, “Theory of a competitive spin liquid state for weak mott insulators on the triangular lattice,” *Phys. Rev. Lett.* **111**, 157203 (2013).
- <sup>57</sup> Samuel Bieri, Claire Lhuillier, and Laura Messio, “Projective symmetry group classification of chiral spin liquids,” *Phys. Rev. B* **93**, 094437 (2016).
- <sup>58</sup> Seiji Yunoki and Sandro Sorella, “Two spin liquid phases in the spatially anisotropic triangular heisenberg model,” *Phys. Rev. B* **74**, 014408 (2006).
- <sup>59</sup> M. Q. Weng, D. N. Sheng, Z. Y. Weng, and Robert J. Bursill, “Spin-liquid phase in an anisotropic triangular-lattice heisenberg model: Exact diagonalization and density-matrix renormalization group calculations,” *Phys. Rev. B* **74**, 012407 (2006).
- <sup>60</sup> Oleg A. Starykh and Leon Balents, “Ordering in spatially anisotropic triangular antiferromagnets,” *Phys. Rev. Lett.* **98**, 077205 (2007).
- <sup>61</sup> Andreas Weichselbaum and Steven R. White, “Incommensurate correlations in the anisotropic triangular heisenberg lattice,” *Phys. Rev. B* **84**, 245130 (2011).
- <sup>62</sup> Ryui Kaneko, Satoshi Morita, and Masatoshi Imada, “Gapless spin-liquid phase in an extended spin 1/2 triangular heisenberg model,” *Journal of the Physical Society of Japan* **83** (2014).
- <sup>63</sup> P. H. Y. Li, R. F. Bishop, and C. E. Campbell, “Quasiclassical magnetic order and its loss in a spin- $\frac{1}{2}$  heisenberg antiferromagnet on a triangular lattice with competing bonds,” *Phys. Rev. B* **91**, 014426 (2015).
- <sup>64</sup> Zhenyue Zhu and Steven R. White, “Spin liquid phase of the  $s = \frac{1}{2} j_1 - j_2$  heisenberg model on the triangular lattice,” *Phys. Rev. B* **92**, 041105 (2015).
- <sup>65</sup> Wen-Jun Hu, Shou-Shu Gong, Wei Zhu, and D. N. Sheng, “Competing spin-liquid states in the spin- $\frac{1}{2}$  heisenberg model on the triangular lattice,” *Phys. Rev. B* **92**, 140403 (2015).
- <sup>66</sup> S. N. Saadatmand and I. P. McCulloch, “Symmetry fractionalization in the topological phase of the spin-1/2  $j_1 - j_2$  triangular heisenberg model,” *Phys. Rev. B* **94**, 121111 (2016).
- <sup>67</sup> Yasir Iqbal, Wen-Jun Hu, Ronny Thomale, Didier Poilblanc, and Federico Becca, “Spin liquid nature in the heisenberg  $j_1 - j_2$  triangular antiferromagnet,” *Phys. Rev. B* **93**, 144411 (2016).
- <sup>68</sup> Joseph AM Paddison, Marcus Daum, Zhiling Dun, Georg Ehlers, Yaohua Liu, Matthew B Stone, Haidong Zhou, and Martin Mouri-gal, “Continuous excitations of the triangular-lattice quantum spin liquid ybmggao<sub>4</sub>,” *Nature Physics* (2016).
- <sup>69</sup> T. Dey, M. Majumder, J. C. Orain, A. Senyshyn, M. Prinz-Zwick, F. Bert, P. Khuntia, N. Büttgen, A. A. Tsirlin, and P. Gegenwart, “Gapless quantum spin liquid ground state in mixed-valence iri-date Ba<sub>3</sub>InIr<sub>2</sub>O<sub>9</sub>,” ArXiv e-prints (2017), arXiv:1702.08305 [cond-mat.str-el].
- <sup>70</sup> W. Zheng, J.-W. Mei, and Y. Qi, “Classification and Monte Carlo study of symmetric  $Z_2$  spin liquids on the triangular lattice,” ArXiv e-prints (2015), arXiv:1505.05351 [cond-mat.str-el].
- <sup>71</sup> Yuan-Ming Lu, “Symmetric  $Z_2$  spin liquids and their neighboring phases on triangular lattice,” *Phys. Rev. B* **93**, 165113 (2016).
- <sup>72</sup> N. Y. Yao, M. P. Zaletel, D. M. Stamper-Kurn, and A. Vishwanath, “A Quantum Dipolar Spin Liquid,” ArXiv e-prints (2015), arXiv:1510.06403 [cond-mat.str-el].
- <sup>73</sup> Wen-Jun Hu, Shou-Shu Gong, and D. N. Sheng, “Variational monte carlo study of chiral spin liquid in quantum antiferromagnet on the triangular lattice,” *Phys. Rev. B* **94**, 075131 (2016).
- <sup>74</sup> Alexander Wietek and Andreas M. Läuchli, “Chiral spin liquid and quantum criticality in extended  $s = \frac{1}{2}$  heisenberg models on the triangular lattice,” *Phys. Rev. B* **95**, 035141 (2017).
- <sup>75</sup> Kazuma Misumi, Tatsuya Kaneko, and Yukinori Ohta, “Mott transition and magnetism of the triangular-lattice hubbard model with next-nearest-neighbor hopping,” *Phys. Rev. B* **95**, 075124 (2017).
- <sup>76</sup> Diptiman Sen and R. Chitra, “Large-u limit of a hubbard model in a magnetic field: Chiral spin interactions and paramagnetism,” *Phys. Rev. B* **51**, 1922–1925 (1995).
- <sup>77</sup> Olexei I. Motrunich, “Orbital magnetic field effects in spin liquid with spinon fermi sea: Possible application to  $\kappa$ -( $\text{ET}$ )<sub>2</sub> $\text{Cu}_2$ ( $\text{CN}$ )<sub>3</sub>,” *Phys. Rev. B* **73**, 155115 (2006).
- <sup>78</sup> Steven R. White, “Density matrix formulation for quantum renormalization groups,” *Phys. Rev. Lett.* **69**, 2863–2866 (1992).
- <sup>79</sup> IP McCulloch and M Gulácsi, “The non-abelian density matrix renormalization group algorithm,” *Europhysics Letters* **57**, 852–858 (2002).
- <sup>80</sup> Weihong Zheng, John O. Fjærestad, Rajiv R. P. Singh, Ross H. McKenzie, and Radu Coldea, “Excitation spectra of the spin- $\frac{1}{2}$  triangular-lattice heisenberg antiferromagnet,” *Phys. Rev. B* **74**, 224420 (2006).
- <sup>81</sup> Steven R. White and A. L. Chernyshev, “Neél order in square and triangular lattice heisenberg models,” *Phys. Rev. Lett.* **99**, 127004 (2007).
- <sup>82</sup> L. Messio, C. Lhuillier, and G. Misguich, “Lattice symmetries and regular magnetic orders in classical frustrated antiferromagnets,” *Phys. Rev. B* **83**, 184401 (2011).
- <sup>83</sup> Hui Li and F. D. M. Haldane, “Entanglement spectrum as a generalization of entanglement entropy: Identification of topological order in non-abelian fractional quantum hall effect states,” *Phys. Rev. Lett.* **101**, 010504 (2008).
- <sup>84</sup> L. Cincio and G. Vidal, “Characterizing topological order by studying the ground states on an infinite cylinder,” *Phys. Rev. Lett.* **110**, 067208 (2013).
- <sup>85</sup> Michael P. Zaletel, Roger S. K. Mong, and Frank Pollmann, “Topological characterization of fractional quantum hall ground states from microscopic hamiltonians,” *Phys. Rev. Lett.* **110**, 236801 (2013).
- <sup>86</sup> Philippe Francesco, Pierre Mathieu, and David Sénéchal, *Conformal field theory* (Springer Science & Business Media, 2012).
- <sup>87</sup> Eduardo Fradkin, Steven A Kivelson, Michael J Lawler, James P Eisenstein, and Andrew P Mackenzie, “Nematic fermi fluids in condensed matter physics,” *Annu. Rev. Condens. Matter Phys.* **1**, 153–178 (2010).
- <sup>88</sup> S. N. Saadatmand and I. P. McCulloch, “Detection and characterization of symmetry-broken long-range orders in the spin- $\frac{1}{2}$  triangular heisenberg model,” *Phys. Rev. B* **96**, 075117 (2017).